Evaluating water-repellents applied to brick masonry: An experimental study by thermal imaging and water transport properties' characterization

Evaluating water-repellents applied to brick masonry: an experimental study by thermal imaging and water transport properties' characterization

Ester Barbieri[1], Francesca Trevisol[1], Cesare Pizzigatti[2], Gabriele Bitelli[1], Elisa Franzoni[2,*]

[1] Department of Civil, Chemical, Environmental and Materials Engineering (DICAM), University of Bologna, Viale del Risorgimento 2, 40136 Bologna, Italy

[2] Department of Civil, Chemical, Environmental and Materials Engineering (DICAM), University of Bologna, Via Terracini 28, 40131 Bologna, Italy

Abstract

Moisture is one of the main problems that affect new and historic masonry buildings, which are the most common ones in Europe and worldwide. The application of surface treatments based on water-repellents is a very common solution to protect masonry from rain and hence from moisture-related problems. However, there are very few studies on the monitoring of water-repellents in real buildings and a deeper knowledge would be necessary on the long-term effectiveness and compatibility of water repellents, especially considering that defects and flaking issues are often reported in-the-field. In this paper, infrared thermography was proposed as a totally non-invasive technique to monitor the behaviour of brick masonry subjected to wetting, both from outside (rain) and inside (internal moisture). An active thermal approach was used to simulate internal and external wetting. The behaviour of the masonry during wetting and drying was investigated both in laboratory walls and in brick samples, to elucidate their water transport properties. All the materials were tested both in untreated conditions and after the application of two different hydrophobic coatings. The results show that the drying behaviour of treated masonry materials is a critical issue, as the coatings may strongly slow down the drying of internal moisture, even if the coefficient of resistance to water vapour diffusion of the products is very low. The results also suggest that the methodology used to process thermal images using multi-temporal analysis is a promising way to interpret the water transport in treated walls and to monitor real buildings where water-repellents were applied.

Keywords: Coating; capillary absorption; vapour diffusion; mortar; brick; infrared; Change Detection analysis; Principal Component Analysis

1. Introduction

Moisture is involved in basically all the deterioration mechanisms affecting masonry materials, so the application of water-repellents that increase the water contact angle and thus prevent the spontaneous

* Corresponding author, elisa.franzoni@unibo.it

capillary absorption of rain is regarded as a quick and successful route to protect the façades of new and historic buildings. Water repellents are surface treatments usually based on alkoxysilanes, silicones, and fluoropolymers, which are applied over building materials to prevent the absorption of liquid water [1]. Many water repellent formulations are available in the market since the 1960s [2], and they are expected to fulfil a range of requirements in terms of effectiveness (water contact angle >90°, uniform protection of the surface), compatibility (limited colour alteration, high water vapour permeability) and durability (long-term effectiveness and absence of incompatible residues). Research is continuously evolving towards the development of new formulations, for example with improved performance and zero VOC emission (among the others, [3] and [4]).

Despite the high number of products, the numerous studies carried out so far highlighted that the final properties achieved through the application of water-repellents can be very different, as they depend on many factors, such as the penetration depth of the treatment [5], the application procedure and the skillfulness of workmanship [6], the characteristics of hydrophobic materials alone [7] and in combination with the substrate on which they are applied [8-9]. Controversial results are often presented and there are still many open questions that need to be answered before it can be concluded that any water-vapor-permeable coatings will improve the durability of masonry [10]. For example, the nature of the mortar joints was reported to have a critical role, hence careful consideration should be given before applying water-repellents to masonry, especially in countries with much driving rain followed by frequent freeze-thaw cycles [11]. In many cases, defects and problems were reported [12] and, according to some authors, further research is needed to understand the mechanisms of failure of hydrophobic treatments [13]. According to the available literature, the possible limitations of water-repellents applied to highly porous materials seem to be mostly the reduction of the drying speed of masonry [8-9], the negative behaviour in case of salt crystallization cycles [14-17] and a limited durability. In particular, the long-term behaviour and efficiency of water-repellents has not yet been systematically studied and completely understood [8, 18] and are still a scientific issue [19]. The available studies report different durations depending on the materials and exposure, ranging from few years (4 [18], or 5-10 years [20-21]) to some decades [2, 19, 22], and there is very little experience in the literature about the durability of the hydrophobic treatment of brick masonry and brick and mortar samples [23].

These studies point out the need of a more extensive and accurate monitoring of hydrophobic treatments applied to real buildings (especially masonry walls) with different exposure, aiming at assessing their performance and scheduling cyclical interventions [24].

Infrared Thermography (IRT) has been widely used since some decades in the monitoring of existing and historical buildings, for a range of purposes [25-27]. IRT is a non-destructive imaging technique that allows to detect the radiation in the infrared spectrum. Electromagnetic radiation is emitted by all bodies having a temperature higher than absolute zero [28], and thermal cameras allow to convert this energy into an electronic signal which is processed to produce a thermal image. Thermography is able to collect information about the presence of moisture in in buildings and historic masonry structures [29-30], allowing to create moisture maps [31-33]. This technique can detect areas affected by moisture accurately, also in presence of small thermal contrasts, however it also exhibits some limitations [34], hence it is often combined with other non-destructive tests [35-37], or an active approach is recommended [34]. In some studies, thermography was employed for the detection of the water evaporation flow in buildings [38], for the non-destructive evaluation of the performance and

compatibility of restoration and repair materials [39], and for the evaluation of the performance of water repellents used in the protection of architectural surfaces [40-41].

The present work proposes a multidisciplinary approach integrating laboratory tests on samples, active thermography and image processing to evaluate the hydric behaviour of brick masonry with and without hydrophobic treatments. The study was carried out in steps. Firstly, the effectiveness and compatibility of two different water repellents was investigated using brick samples, by assessing the hydric behaviour of treated bricks during wetting and drying, compared to untreated ones. Particular care was given to evaluate how the evaporative drying behaviour is influenced by the presence of the treatments and to compare the results with the coefficients of resistance to water vapour diffusion determined through the standard wet cup method. The results showed that there is a huge difference, suggesting that the standard test overestimates the evaporation of water through water repelling surfaces. Secondly, two brick walls were built in laboratory and a novel experimental set-up was designed to reproduce the conditions of wetting and drying that are experienced by real masonry in the field, including the evaporation of the internal moisture present behind the treated surface (i.e., moisture deriving from condensation and/or infiltration). In this case, the behaviour of treated and untreated brick walls was investigated by acquiring thermal images during the experiment, following the phases of wetting and drying of the walls in different conditions. In this way, thermography was employed according to active approach. While passive thermography just captures the image, active thermography uses an external action to trigger a reaction from the material, hence it allows to investigate conditions that are not detectable with passive thermography. The reaction sparked by the external agent (water, in this case) can be studied and analysed by acquiring thermal images over a period. Having a set of thermal images that describe over time the evolution of the surface temperature of the material allows to use different image processing techniques. Indeed, the image processing techniques, such as change detection, are crucial to extract valuable information from multitemporal IRT dataset. Change Detection Analysis (CDA) refers to identify modification occurred during time over the investigated surface. In the context of image processing, CDA is performed by comparison of the same scene acquired at different time. This approach is commonly used in a variety of field such as remote sensing [42], medical diagnosis and treatment [43] and civil infrastructure. In the context of remotely sensed data, as summarized by [44], standard change detection (CD) methods can be categorized in three main groups: (1) image enhancement methods, (2) multitemporal analysis, and (3) post classification comparison. Image enhancement methods mathematically transform unclassified images acquired at different time to enhance information, examples are image-differencing, image-rationing, principal component analysis. The Principal Component Analysis (PCA) is a common transformation technique for reducing the dimensionality of datasets, increasing interpretability and minimizing information loss [45]. PCA is a mathematical transformation that calculate the covariance matrix of the original feature space in order to obtain eigenvalue. Applying a linear transformation to the original feature space, obtained from the eigen vectors of the covariance matrix, a new orthogonal co-ordinate system can be defined [46]. Principal component images corresponding to higher eigenvalue (first component) reflect high correlation between the original data, which identify unchanged areas over the images. On the other hand, principal components corresponding to smaller eigenvalues highlight changed parts of the images [47]. A CDA involving the PC analysis helps to highlight areas over the image where change occurred and further investigations are necessary. In the context of building materials, it was shown that change detection

analysis represents a powerful technique to extract valuable information from a large set of thermal images, otherwise not easily manageable. Among other techniques, PCA has been proven to highlight patterns in thermal IRT datasets enabling defect detection in different materials and conditions [48-50].

In this study, the combination of thermal imaging and its processing by CDA with laboratory tests on brick and wall samples allowed to collect information on the hydric behaviour of water-repellents applied to brick masonry and contributed to the application of thermography to the long-term monitoring of treated masonry buildings.

2. Materials and methods

2.1 Overview of the research

The work was carried out in three main phases: tests on brick samples, thermal imaging of brick walls using an active approach, tests on samples collected from the brick walls (Figure 1). The first phase was aimed at evaluating the effectiveness and compatibility of two treatments, focusing on the hydric behaviour of treated and untreated bricks (absorption due to external wetting; evaporation of internal moisture), and to collect data for the following phase of active IRT and PC analysis. During the second phase, small masonry walls were treated with the same two treatments and subjected to internal and external wetting, according to the approach used in the first phase, and the absorption and drying behaviour was monitored during several days by IRT, using the PC analysis to investigate those changes that cannot be detected in thermal images alone. In the last phase, samples were core drilled from the walls and tested, for a check of the consistency of the results with those obtained in the first phase.

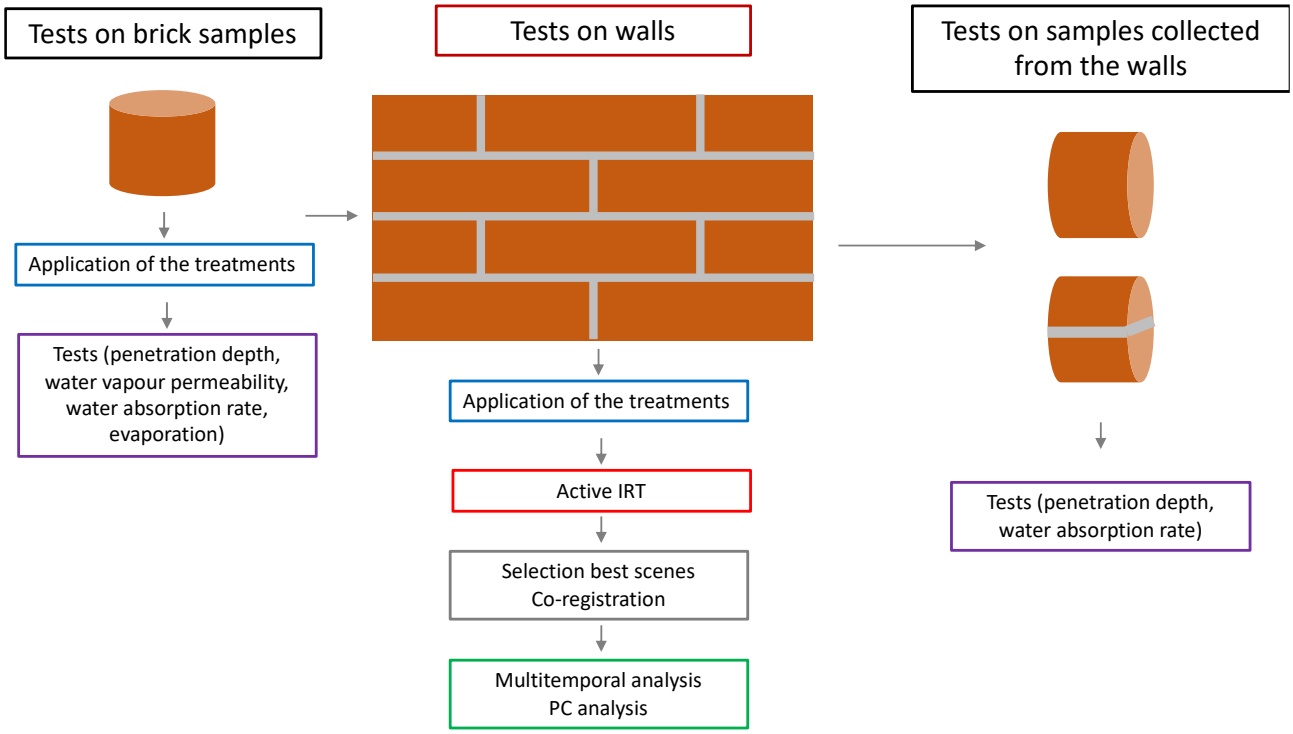

Figure 1. Main phases of the study.

2.2 Tests on brick samples

Commercial solid bricks (size 24.5×11×5.5 cm^3), having bulk density 1756 ± 11 kg/m^3, and water absorption 16.4 ± 0.1 wt%, were used in the laboratory tests. Ten cylindrical samples (diameter = 55 mm, height = 18 mm) were obtained by perpendicularly core drilling one single brick.

Two different water repellents were used in this study, considered as representative of hydrophobic treatments widely used in historic buildings. The first one is a solvent-free emulsion of silane-siloxane in water (solid content 50%, density 0.95 kg/l, Aquasil) and was labelled as treatment "A", while the second one is constituted by polysiloxane dissolved in white spirit (density 0.81 kg/l, Idrosil) and was labelled as treatment "B".

The treatments (A and B) were applied on one circular face, by brushing and by spraying, labelling the samples as in the following:

- (A or B)-BRU-1, sample treated with 1 brushstroke
- (A or B)-BRU-2, sample treated with 2 brushstrokes
- (A or B)-SPR-1, sample treated with 1 spray
- (A or B)-SPR-2, sample treated with 2 sprays.

Two samples (UT) were left untreated, for comparison. All the cylinders used for the tests were obtained from one single brick, allowing to avoid any variability among bricks, which is a critical issue in any experimental campaign involving this type of material. One sample was used for each treatment and condition, because it was considered that a direct comparison of the treatments was possible, belonging all the samples to the same brick.

The mass increase of each sample immediately after the application of the treatments was measured by weighing the cylinders. After the treatments' application, the samples were let dry and

cure for one week at laboratory conditions. Then, the treated and untreated samples were subjected to four different tests (Figure 2).

- Determination of the capillarity absorption rate
- Determination of the capillarity absorption after artificial rain
- Determination of the coefficient of resistance to water vapour diffusion
- Determination of the drying rate in case of internal moisture.

The water capillary absorption rate was measured according to EN 15801 [51], putting the sample in contact with wet filter paper (treated face down). After the test, the samples were let dry at laboratory condition up to constant weight, and then they were used for the determination of the capillary absorption by spraying, i.e., in conditions simulating a rainfall event. In this case, all the surfaces of the cylinders were sealed with Parafilm, except for the treated one. Deionized water was sprayed perpendicular to the treated surface (kept in vertical position) for 10 times, for a total water amount corresponding to 5.6 mm of rain. At the end of the spraying, the droplets of water on the surface were gently removed with a wet tissue and the mass of the samples was measured, to calculate the amount of water absorbed. After the test, the sealing films were removed and the samples were let dry at laboratory condition up to constant weight. Therefore, the samples were put in contact with wet filter paper (treated face up) and let absorb deionized water up to constant mass, indicating that saturation was achieved. The saturation by capillary absorption was considered to better reproduce the occurrence of internal moisture in real building materials [52], with respect to saturation by immersion proposed in other standards [53-54]. At this moment, all the surfaces were immediately sealed with Parafilm and duct tape, except the treated one, and they were let dry (through the treated face only) at laboratory conditions (temperature 21 °C, relative humidity 45%), measuring their mass at fixed intervals. The first and the second drying rates (in g/m^2h and $g/m^2h^{1/2}$, respectively) were calculated from the drying curves, according to EN 16322 [54]. After drying the samples at laboratory conditions, they were finally used for the determination of the coefficient of resistance to water vapor diffusion, by the wet cup method, according to EN ISO 12572 [55] and EN 1015-19 [56] standards. A saturated aqueous solution of potassium nitrate was used to keep the air relative humidity inside the cup equal to 94%.

After the tests, the brick cylinders were broken along their length and the penetration depth of the hydrophobic treatment was visually assessed, by spraying some water on the cross-section and observing the darkening of the untreated brick (hydrophilic).

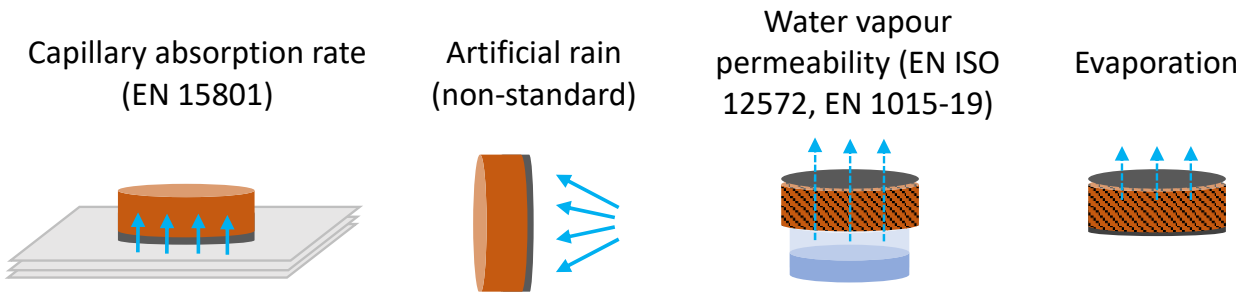

Figure 2. Schematic representation of the tests on brick cylinders (the grey layer represents the hydrophobic coating). The use of parafilm and duct tape ensured the removal of the sealing without residues on the surface and allowed to perform all the four tests exactly on the same samples.

Water vapour permeability is particularly important in historic buildings, where porous materials such as brick, stone and renders are present, because the evaporation of the moisture possibly trapped behind the coating must be allowed. Otherwise, flaking and detachment of the coating may occur, with detrimental effects. Despite the wide use of water repellents in historic buildings and the number of laboratory studies on their performance and compatibility in different materials, little is still known about their actual behaviour when applied to existing façades, especially after some years of outdoor exposure.

2.3 Tests on brick masonry walls

Two identical brick masonry walls (50×25×10.5 cm^3) were built in laboratory using the same bricks used in Section 2.2 and a natural hydraulic lime-based mortar. The mortar was prepared using 1350 g of sand, 356 g of natural hydraulic lime, and 340 g of water. Mortar joints having thickness 1.5 cm were adopted. The walls were labelled as "wall 1" and "wall 2" and left to cure in laboratory conditions for 4 months.

Horizontal holes having diameter 1 cm were drilled from the back of the walls, in correspondence of mortar joints and bricks, respectively. The length of the holes was equal to the thickness of the walls minus 2 cm. Flexible pipes connected to funnels were inserted in the holes and sealed, allowing the injection of water just behind the front surface of the wall. This was done to simulate the presence of water just behind the external surface of masonry, which is a common occurrence in real buildings. In fact, rain may infiltrate inside the masonry through cracks and voids (e.g., in correspondence of brick/mortar interfaces, windowsills, etc.) or from roof leakage, and moreover water may form due to internal condensation. In any case, the masonry may experience the presence of moisture, meaning liquid water, inside it. The funnels and pipes allow to artificially introduce a desired amount of water inside the wall and specifically a couple of cm below the external surface, allowing to investigate the evaporation behaviour.

Some preliminary tests were carried out before the application of the water repellent treatments, aiming at investigating the drying behaviour of the masonry walls. Water was poured from the rear of the walls through the funnels and pipes inserted in advance, to check the feasibility of the internal wetting procedure designed in this study and to observe how water evaporates in absence of surface treatments. The procedure was repeated two times and the results were also taken as reference for the following tests on the water repellents.

After complete drying, the hydrophobic treatments were applied. The left half of wall 1 was treated with water repellent B, while the left half of wall 2 was treated with water repellent A (Figure 3). The water repellents were applied by 2 brushstrokes and left cure for at least 1 week before any test.

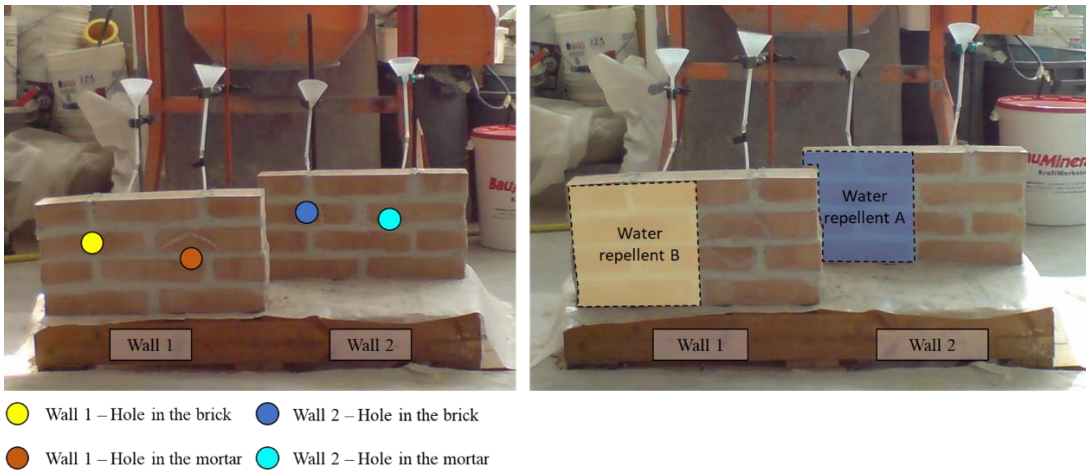

Figure 3. On the left: positions of holes drilled from the back face of the walls (not visible on the front surface). On the right: areas treated with the two water-repellents (black dashed).

The study was conducted at three different stages, using active IR thermography to investigate the wetting and evaporation behaviour of water in the walls in different conditions.

The infrared camera used for this study was the FLIR P620, mounted on tripod. FLIR P620 works in the spectral electromagnetic domain of 7.5–13 µm, with a standard temperature range from -40 °C to 500 °C. FLIR P620 has a thermal sensitivity of 40 mK and produces infrared images with a resolution of 640 x 480 pixels. Three significant sets of acquisitions were collected, in the following conditions (Table 1):

I - Internal wetting (through the funnels and pipes), before the water repellent application

II - Internal wetting through the same procedure described above, after the water repellent application

III - External wetting of the front surface by spraying, after the water repellent application.

Deionized water was used in all the tests (T=15-17°C). In test I, the temperature differences due to water evaporation detected by IRT were very small, hence during the following tests (II and III) all the surfaces of the walls except the front one were covered with plastic film and duct tape, so to ensure that evaporation occurred only through the front surface, maximising the cooling effect detectable by IRT and better simulating real buildings where thick masonry walls are present.

Table 1. Information on thermal imaging days.

Test #	*Condition*	*Acquisition date*	*T (°C)*	*RH%*	*Type of test*
I	Before the treatment	09/18/2020	26.6	64	**Internal wetting (by funnels and pipes)**
		09/23/2020	24.4	63	Drying, evaporation possible from all the surfaces
		09/25/2020	25.2	61	Drying, evaporation possible from all the surfaces
II	After the treatment	02/02/2021	19.4	37	**Internal wetting (by funnels and pipes)**
		02/03/2021	19.1	34	Drying, evaporation possible only through the front surface
		02/05/2021	19.5	46	Drying, evaporation possible only through the front surface
		02/08/2021	20.9	41	Drying, evaporation possible only through the front surface
III	After the treatment	02/10/2021	21.6	46	**External wetting (by spraying)**
		02/11/2021	20.9	39	Drying, evaporation possible only through the front surface
		02/12/2021	21.1	30	Drying, evaporation possible only through the front surface

In test I, both untreated walls were subjected by internal wetting, by gradually pouring 500 ml of deionized water in each of the four funnels by a pipette and letting the masonry to completely absorb it. This pouring operation lasted about 2 hours. The first set of images was acquired over three days. The wetting and drying phases were documented at day 1, 5 and 7 from wetting. After drying, the walls were treated with water repellents A and B, as described above and let cure.

In test II, which was carried out after the treatments' application as in Fig. 3, the internal wetting was repeated in the same way as in the first test, i.e., by pouring 500 ml of deionized water into each of the four holes. Thermal images were taken over a period of six days to assess the rate of water evaporation through the surfaces of concern. From the 40 images acquired, 12 most representative images were chosen to describe the main phases of the experiment, also excluding the images in which some disturbance from the environment (due to windows and doors) affected the thermal behaviour of the walls. As described above, all the wall surfaces were wrapped with plastic film and duct tape except for the front surface (half treated and half untreated), to make evaporation possible only through it.

Test III was carried out 8 days after the previous test, when drying was considered complete (based on IRT and on what found on brick samples, in section 3.1). In this test, the walls were wetted from the external side, simulating rainfall. Ten consecutive cycles of spraying were carried out, resulting in an overall amount of 700 ml of deionized water for each wall, equivalent to 5.6 mm of rain height, representative of a medium-intensity rainfall in the area of Bologna (dataset Eraclito4, ARPAE – Agenzia Regionale per la Prevenzione, l'Ambiente e l'Energia, Emilia-Romagna) [57]. Also in this case the evaporation was possible only through the front surface, which was the only one unwrapped. The water amount was the same be used for the wetting of brick samples in Section 2.2.

At the end of each test, thermal images were processed using FLIR software, which allows to set the acquisition parameters (atmospheric temperature, relative humidity, distance from the object) and produce tiff files at 32-bit.

2.4 IRT Image processing

To be able to compare images of the same test, having been taken on several days, it is necessary to edit them. As the thermal camera did not stand fixed on all acquisition days from wetting to drying, the images had to be co-registered to have a perfect pixel match. The images of the same set were co-registered in the same local reference system, so that a pixel-based analysis could be carried out later.

Firstly, pre-processing is needed to ensure the procedure detects only changes due to thermic variation, reducing (other) disturbance factors, such as changes in temperature and lighting in the lab where the experiment was conducted. In fact, having acquired the thermal images over time, at certain times of the day the images record a temperature variation due to external agents.

A stack of all selected images for each set was produced, which allows the extraction of the time-series of temperature for each pixel.

Extracting the temperature time series from different zone (treated/untreated) of the walls allows to evaluate the response of the two water-repellents to different 'stress' conditions. To make the representation of temperature differences acquired during the study more intuitive, the TIR images

have been corrected taking as reference the average of the values of the pixels before the wetting. In this way, the deviation from a moment T_0 that represents the dry wall before the start of the tests is evident.

A change detection analysis based on PCA (Principal Component Analysis) was performed to highlight areas where the wetting/drying phases caused a higher change of the temperature over the wall surface (Figure 4). This approach was considered highly suitable for extracting information of temperature changes over surface from a consistent number of thermal images. Through the co-registered stack of thermal images, the original feature space was created: each pixel is described by a vector collecting the temperature time series. The covariance matrix was calculated for each set to extract the eigenvalues that were used to produce the principal component images. Only the first four components were considered significant for the study. As described above, the principal component images corresponding to large eigenvalues are assumed to reflect the unchanged part of the images, and those corresponding to smaller eigenvalues to changed parts of the images.

The first component images contain no-change pixels whereas the second, third and fourth component images contain change information between different acquisition times.

This analysis allows to point out areas for further investigation, extracting information on spatial and temporal evolution of temperature over those parts of the walls via transects.

Another way to highlight changes occurred over time in the acquired dataset can be found in image visualization techniques. For example, the RGB composite technique can be used for this purpose. Indeed, in the RGB colour space, a colour can be expressed by a combination of the primary components red, green and blue and visualized in an n-bit display system [58]. In this way, assigning the red, green and blue channels respectively to acquisitions referring to different times or states, a single composite image is produced, where the final colour of each pixel is representative of changes occurred. In this case, the principal component images were used as input in the procedure (Figure 5). For example, a pixel displayed in yellow in the composite image is referred to relative high values in the PC_i (red) and PC_j (greed) components but low values in the PC_k (blue).

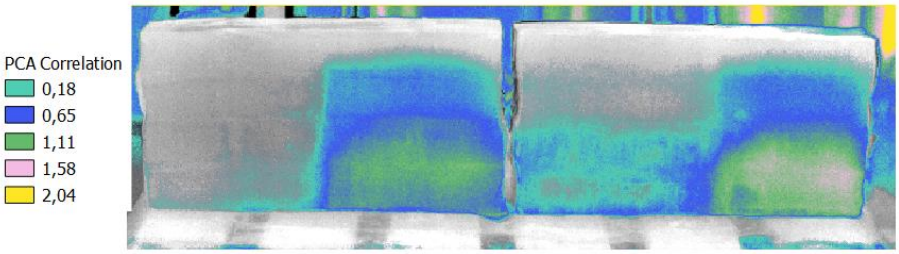

Figure 4. PCA second component: this visualisation highlights the areas where there was the most variation during the experiment.

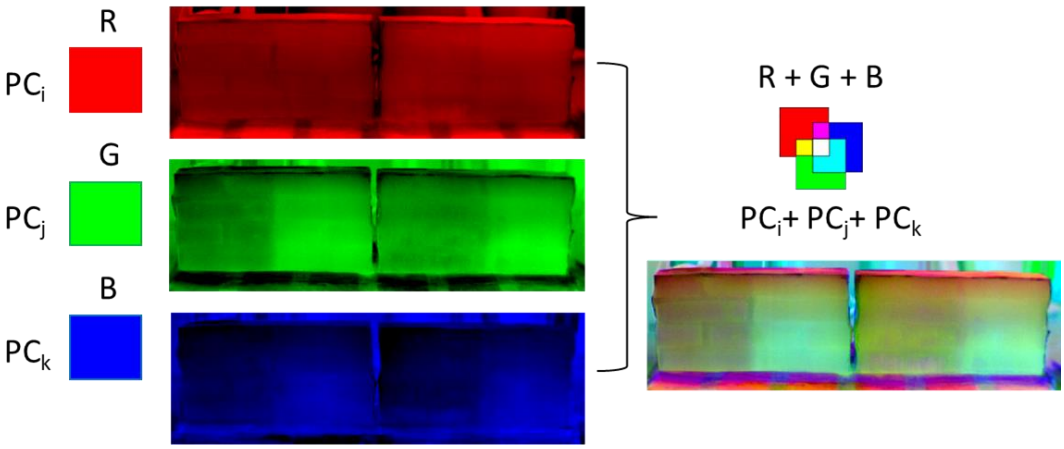

Figure 5. RGB multi-band visualisation scheme.

2.5 Tests on samples core-drilled from the brick walls

After the conclusion of the tests on brick walls, six cylinders having diameter 5 cm and thickness ~7 cm were core drilled from each of them, perpendicular to the front face. The cylinders were constituted by brick only or by brick and mortar joint. Two samples were collected from the untreated part, whereas the remaining four samples were collected from the treated part, as shown in Figure 6.

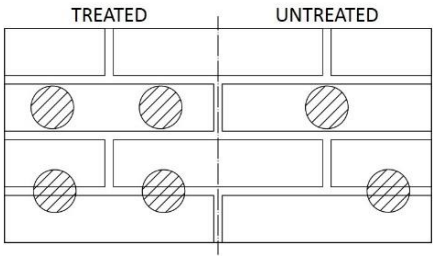

Figure 6. Scheme of collection of the six cylindrical samples from each wall

The cores constituted by brick only were subjected to water capillary absorption test from the treated surfaces, aiming at a comparison with the results obtained for brick cylinders described in Section 2.2. The same testing procedure previously described was used. These cores were labelled: 1-UT and 2-UT (samples collected from the untreated parts of wall 1 and wall 2, respectively), 2-A-a and 2-A-b (samples collected from wall 2, in the area treated with the “A” product), 1-B-a and 1-B-b (samples collected from wall 1, in the area treated with the “B” product).

Afterwards, all the 12 cylinders were dried at room conditions and then sprayed with deionized water. The penetration depth of the treatments was visually assessed by observing the dark, wet part on the lateral surface. In the samples constituted by brick and mortar, the penetration depth was observed separately on the mortar layer and the brick.

3. Results and discussion

3.1 Tests on brick samples

The mass increase of the brick samples due to the treatments' application is reported in Table 2. Considering that the density of the two water repellents is quite similar and the method of application is the same, the results suggest that brushing slightly favours the uptake of the products with respect to spraying, and that the water emulsion (A) is absorbed in remarkably higher amount than the solution in white spirit (B). This latter observation is confirmed by the penetration depth of the hydrophobic treatments, shown in Figure 7. Product A penetrates many mm in the brick and the second application always induces a higher penetration, for both brushing and spraying. Product B remains basically at the surface, the penetration depth being only 1 mm for all the application procedures. This can be ascribed to the nature of the white spirit solvent, which is very volatile and prevents a deep capillary absorption of the hydrophobic treatment, differently from water, an effect that was highlighted in studies on the penetration depth of conservation products [59-60].

In terms of effectiveness, the absorption of water is drastically reduced thanks to the treatments, both in the standard capillary absorption test and in the test where water was sprayed onto the brick surface kept in vertical position (Table 3). Given the very limited absorption of water by all the treated surface, it was not possible to find clear correlations between the values in Table 3 and the application method.

Table 2. Mass increase due to the treatments' application (mass was measured immediately after the application of the liquid product).

Sample	**Dry mass before the treatment application (g)**	**Mass increase due to the first application**		**Mass increase due to the second application**	
		%	**g/m^2**	**%**	**g/m^2**
A-BRU-1	73.80	0.53	164.2	-	-
A-BRU-2	75.70	0.36	113.7	0.54	172.7
A-SPR-1	80.76	0.28	96.7	-	-
A-SPR-2	76.55	0.21	67.4	0.27	88.4
B-BRU-1	80.50	0.20	67.4	-	-
B-BRU-2	81.51	0.20	67.4	0.17	59.0
B-SPR-1	80.70	0.15	50.5	-	-
B-SPR-2	80.63	0.11	37.9	0.14	46.3

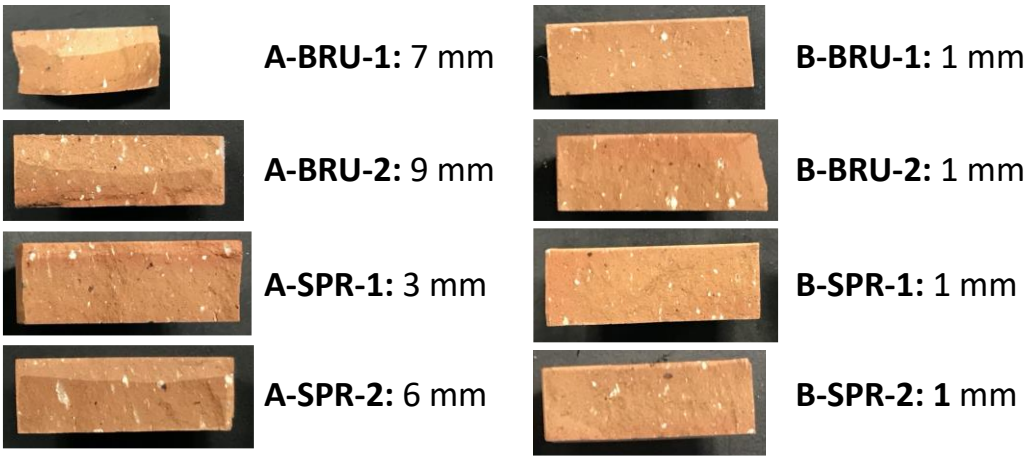

Figure 7. Penetration depth of the hydrophobic treatments observed by wetting the cross section of the bricks.

Table 3. Characteristics of the samples before and after the treatment.

Sample	**Capillary absorption rate ($mg/cm^2s^{1/2}$)**	**Water absorbed after spraying (mg/cm^2)**	**μ (-)**
UT1	25.62	222.35	12
UT2	26.61	163.82	12
A-BRU-1	0.06	1.68	13
A-BRU-2	0.04	1.68	13
A-SPR-1	0.73	28.64	11
A-SPR-2	0.06	1.68	12
B-BRU-1	0.24	12.21	11
B-BRU-2	0.12	1.26	12
B-SPR-1	0.42	5.47	11
B-SPR-2	0.11	2.53	11

The coefficient of resistance to the diffusion of water vapor (μ in Table 3) determined for the untreated brick samples remained basically unaltered after the application of all the treatments, regardless their formulation and penetration depth. The coefficient μ, which is reported in the technical datasheet of any commercial product, is the key parameter currently considered in the restoration practice to evaluate the "breathability" of the treatments and hence to select them, especially for the application to heritage buildings.

The drying curves of the samples are reported in Figure 8, plotting the percentage of moisture in the samples (i.e., mass of water in the samples over their dry mass) during time. The drying curves of untreated samples (UT1 and UT2) exhibit the typical shape of porous building materials, i.e. constituted by two distinct stages, which are well established in the scientific literature [61-62]. The first stage is the constant drying period (when the pore interconnection [63] and the environmental conditions [54, 61-62] mainly influence the drying rate), while in the second stage, identified by the change in the slope of the drying curve, the liquid water can no longer support the demands of the evaporation flux and the drying front recedes progressively into the material. In this second stage, drying occurs in the vapour phase [8]. The drying curves of the samples with the hydrophobic

treatments and the drying indexes calculated according to EN 16322:2013 [54] (Table 4) allow to make the following observations:

- The moisture amount at the beginning of the test obviously depends on the presence and penetration depth of the treatments. For UT samples, this amount was 15.7%, corresponding to the saturation achieved by capillary absorption. In the case of water repellent B, which penetrated 1 mm only, the samples were almost entirely wet, while in the case of water repellent A, which penetrated many mm, the initial moisture content was much lower.
- The drying rate of the brick samples was remarkably reduced after the treatments' application. In the first stage of drying, the reduction was very high for treatment A (-77% on average) and high for treatment B (-41% on average), which reflects the much higher penetration depth of water-repellent A, although the reduction is significant also in treatment B notwithstanding the presence of the water repellent only at the surface. The results are consistent with the fact that in the case of hydrophobic treatment the drying in the first stage is expected to take place only by vapour diffusion [54]. However, interestingly, a strong reduction of the drying rate due to water repellents can be observed also in the second stage, although lower than in the first stage (-63% and -35% on average, for treatments A and B respectively).
- On the whole, the treatments have a strong effect on the drying of the treated materials. For example, after 2 days drying, the untreated bricks exhibited a moisture amount around 3%, while all the treated samples (except A-BRU-2) exhibited a moisture amount between 6 and 8%.

These results clearly indicate that there is a mismatch between the water vapour permeability of the coatings determined by the wet cup method (μ values in Table 3) and the drying behaviour of the treated materials in Figure 8 and Table 4. This is consistent with the findings of other studies, where it was pointed out that the hydrophobic treatments hinder drying and a low correlation was found between μ and the drying index, suggesting that vapour permeability can be an insufficient measure of the effect that water repellents have on drying processes [64]. Moreover, the drying index was found to change with hydrophobic treatments in a different way depending on the substrate materials, namely increasing for limestone and decreasing for mortars, although the water vapour permeability of the treated specimens was not significantly affected by the hydrophobic treatments [8].

In the present tests, one sample per condition was used and the comparability of results was expected to be ensured by the provenance of all the samples from the same brick. However, further tests will be necessary on a high number of samples, to take into account also the heterogeneity among bricks and the possible variability of the application procedure.

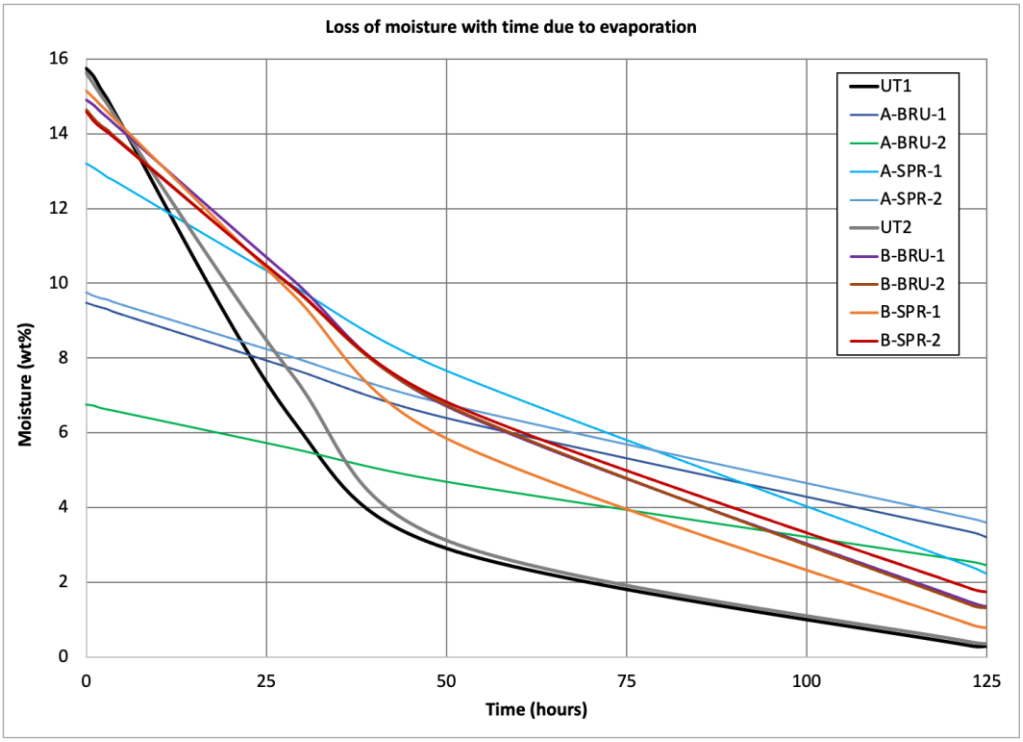

Figure 8. Loss of moisture due to the evaporation of water through one face only (the treated one, for the samples where the water repellents were applied).

Table 4. Drying rates calculated according to EN 16322:2013

Sample	**1st stage drying rate (g/m^2h)**	**2nd stage drying rate ($g/m^2h^{1/2}$)**
UT1	104	765
UT2	93	729
A-BRU-1	19	237
A-BRU-2	13	169
A-SPR-1	38	441
A-SPR-2	19	244
B-BRU-1	57	483
B-BRU-2	56	479
B-SPR-1	65	514
B-SPR-2	55	454

3.2 Tests on brick masonry walls

3.2.1 Thermal images

A high number of thermal images was acquired during the experimental campaign, which were processed by PCA and are discussed in the following. These images are not extensively reported, for brevity's sake, but examples of thermal images acquired during the three phases are reported in Figure 9. In particular, thermal images are reported for: internal wetting (Fig. 9-a) and subsequent drying (Fig. 9-b) before the treatments' application; internal wetting (Fig. 9-c) and subsequent drying (Fig.

9-d) after the treatments' application; external wetting (Fig. 9-e) and subsequent drying (Fig. 9-f) after the treatments' application.

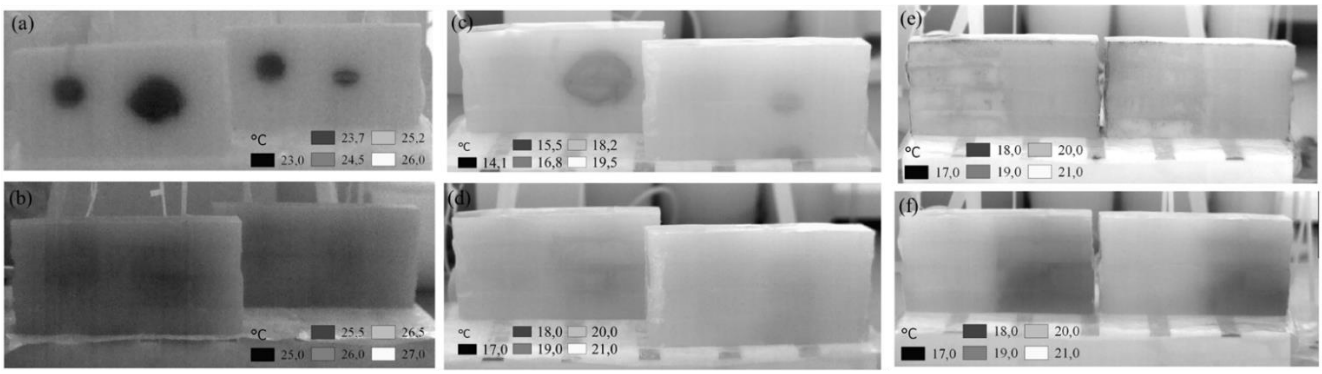

Figure 9. Examples of thermal images taken during the tests. Internal wetting before the treatments' application: during wetting (a) and during drying (b). Internal wetting after the treatments' application: during wetting (c) and during drying (d). External wetting by spraying after the treatments' application: during wetting (e) and during drying (f).

3.2.2 Internal wetting after the water-repellents application

The results of the preliminary tests were very useful to understand the effect of internal wetting carried out on the untreated walls and to follow the subsequent drying. Two thermal images taken at significant times of the procedure are reported in Fig. 9a-b. Fig. 9a refers to the end of the internal wetting procedure (which lasted about 2 hours) and indicates that water introduced inside the bricks (on the left in each wall) reached the front surface as expected and spread quite uniformly in walls 1 and 2, involving also the upper and lower mortar joints. The water poured in the mortars (on the right in each wall) was less uniform and spread more in wall 1 and less in wall 2, likely due to the presence of the brick-mortar interfaces, which may exhibit some microcraks. Notably, in both walls, the water was absorbed also by the adjacent bricks, showing that any evaluation of the internal drying through the mortar joints only was impossible. Hence, in the following, the comparison between bricks and mortar joints was discarded, as the water poured into the bricks spread also to the joints and the water poured into the joints spread also to the surrounding bricks.

From the point of view of drying (Fig. 9a), the preliminary tests showed that this process took more than expected, i.e., about 9 days. The entire sequence of thermal images is not reported here, for brevity's sake. The results obtained after the treatments were compared with the preliminary ones, obtained before the application of the water repellents (Section 3.2.1). The untreated parts exhibited the same behaviour observed before, which confirmed the repeatability of the procedure. In the treated parts, the circular zone affected by wetting reached approximately the same diameter, but the temperature difference between wet and dry zone detected by IRT was much lower than before, suggesting a significant slowing down of the water evaporation (hence, of the cooling effect) due to the water repellents. Notably, the results also show that, despite this, the thermal imaging is able to detect the presence of moisture behind the treated layer, confirming the potential of this technique for onsite monitoring.

3.2.3 Internal wetting after the water-repellents application

To identify the areas subject to the greatest variations, a principal component analysis was carried out. The PCA shows that the areas corresponding to the holes are the most subjected to variation throughout the experiment, as expected. The greatest variation is shown at the hole drilled in the mortar (untreated zone), while the two areas treated with water repellents (where the holes were in the bricks) show a similar variation.

In order to further investigate the behaviour of these zones, a spatio-temporal analysis was carried out using transects (Figure 10). The transects were processed on the layer stuck acquisitions of the wetting and drying phase, which cover a total of seven days. To show the results more clearly, the images were corrected to the initial value. A raster-to-raster operation was carried out, subtracting the first image acquired at time t_1 (just before wetting) from the whole set to compare all values with respect to the dry walls. The graph then shows how the temperature varies with time in space. In the transect the acquisitions at times $t_{1,\ 2,\ 5,\ 7,\ 11,\ 12}$ have been considered, to follow the trend during the whole experiment. t_1 is the initial time, just before wetting, $t_{2,\ 5,\ 7}$ refer to the wetting phase (on the same day), while $t_{11,\ 12}$ refer to the drying phase in the following days. In particular, t_{11} is the acquisition at 72 hours after wetting, while t_{12} is the acquisition at 144 hours after wetting.

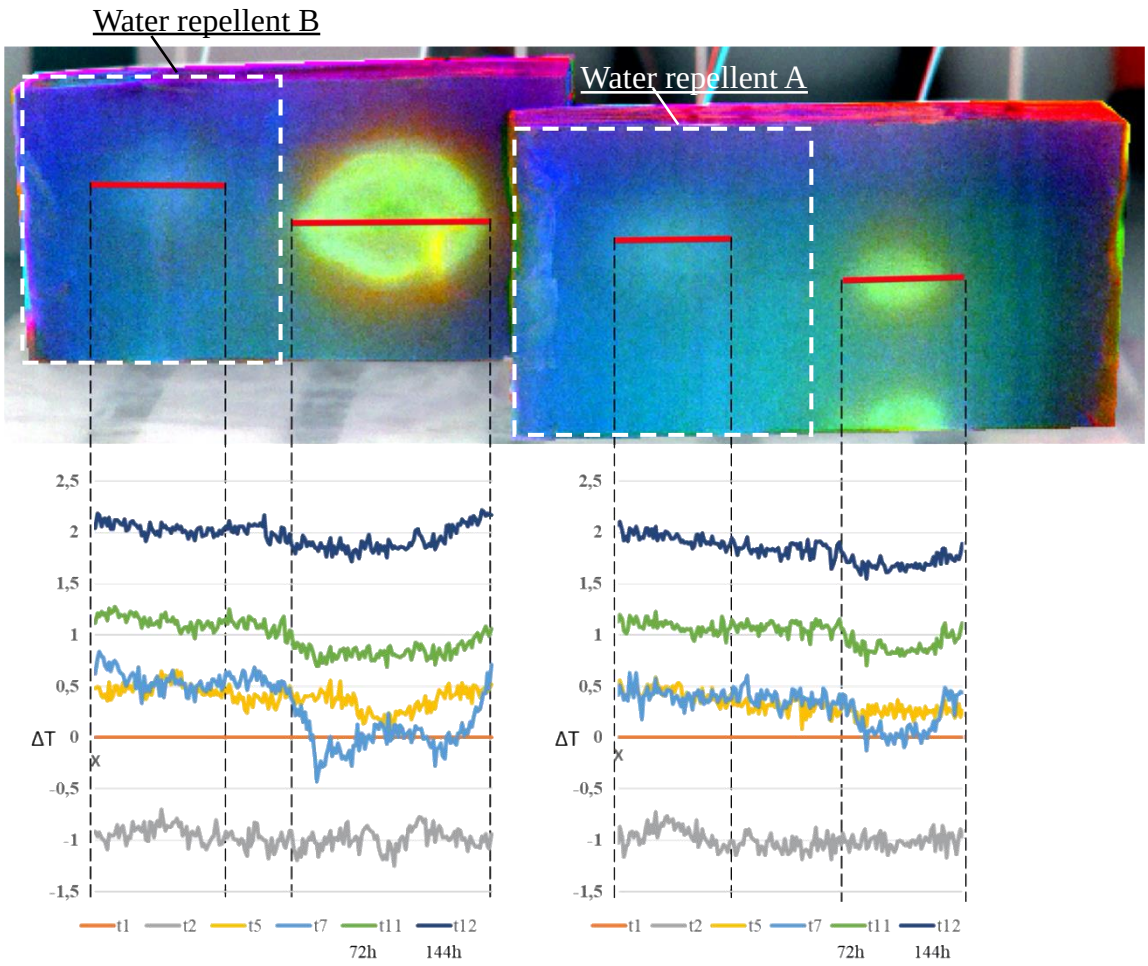

Figure 10. Wall 1 and wall 2 (on the left and right, respectively): thermal transect graphs showing the temperature variation during the acquisition phase in space. The wetting phase ($T_{2,\ 5,\ 7}$) lasted about 3 hours.

The slight lowering of temperature at t_2 was ascribed to the temperature decrease in the laboratory (due to air-conditioning), rather than to the wetting, as the decrease was uniform in both walls and in

all the surface. At time t_5, temperature was slightly lower in the untreated parts, likely due to the use of fresh deionized water (colder than the walls). At time t_7, the difference between treated and untreated transects was very marked, clearly indicating the occurrence of evaporation through the latter. Interestingly, the results indicate that evaporation is still occurring in the untreated parts at t_{11} and t_{12} (3 and 6 days after wetting), although this could not be seen by naked eye. Conversely, evaporation seems strongly hindered in the treated parts (especially in the bricks, where the holes were present), or at least it was so slow not to produce any temperature variation in the walls. The temperature differences between the different days of measurement are likely due to normal climatic variations.

3.2.4 External wetting after the water-repellents application

The second test was carried out spraying the front face of the walls with water. Each wall was divided into two halves through an ideal horizontal line and water was sprayed along each half moving the sprayer from left to right (duration: 12 seconds, distance between nozzle and surface: 20 cm). The spraying operation was repeated 10 times, at intervals of 5 minutes. The wetting by spraying revealed clear differences between the two types of water repellent used and between treated and untreated areas. Also for this second test, the PCA was processed in order to visualise the areas of greatest change.

The space-time analysis was carried out by means of transects. The same procedure described above was used: the set of images used for the space-time analysis was corrected with reference to time t_1 (just before wetting), to compare all the images with respect to the dry value (Figure 11). For the transect, images acquired on the same day of wetting test were considered.

In order to best visualise the transects, acquisitions were chosen which describe the key moments of the experiment ($t_{1, 4, 9, 14, 23, 36}$). The acquisition times $t_{4, 9}$ are related to the wetting phase, while $t_{14, 23, 36}$ are related to the drying phase. The transect was taken at the middle of the wall to evaluate the difference between treated and untreated zones at same acquisition. During the wetting phase ($t_{4, 9}$), the temperature is slightly lower in the treated parts, as the sprayed water (colder than the walls) is retained on the surface rather than being absorbed. On the contrary, during the drying phase, the differences are very marked especially in wall 1, where the untreated part is cold due to evaporation, while in wall 2 the behaviour is more similar in the untreated and treated parts. In fact, differently from wall 1, wall 2 exhibited a high amount of water droplets on the surface at the end of the spraying, hence the IRT detected their evaporation from the surface. In addition, this analysis is also feasible for the identification of materials' physical defects. Indeed, thermal discontinuity along the transect points out the presence of defects that may retain more water than the hydrophobic zone. During the drying phase, a temperature drop is present close to the transition zone in wall 2. This negative peak was ascribed to a non-perfect adhesion between brick and mortar. This physical discontinuity zone, detected by IRT, retains a greater amount of water, which could induce a point of failure in the treatment effectiveness.

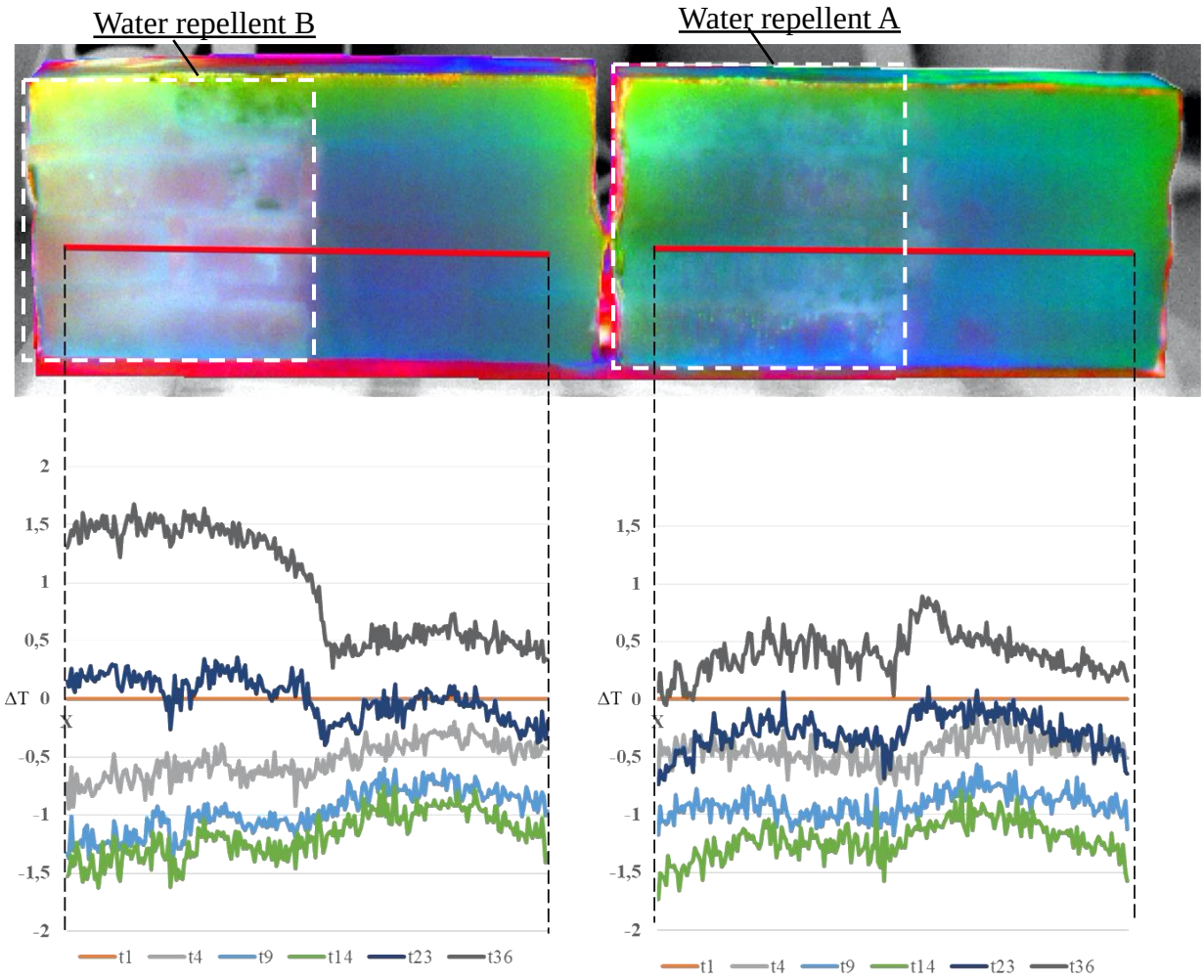

Figure 11. Wall 1 and wall 2 (on the left and right, respectively): temperature evolution in each acquisition, referring to the transects taken as reference area (red lines). Each transect crosses the treated and untreated wall surface.

The external wetting test showed marked differences between treated and untreated areas and between different water repellents. To analyse these differences, the time series of the acquired thermal images were plotted in Figure 12 (the wetting started at time t_2 and lasted about 60 minutes). In the wetting phase, the temperature of wall 1 (Fig. 12, a-b) decreased more in the area treated with water repellent (presence of cold water droplets on the surface), while in the drying phase the curves are reversed (evaporation of water absorbed by the untreated masonry). Drying was still running 48 hours after the wetting (Fig. 12, b). In wall 2, the difference in behaviour between treated and untreated areas was smaller (Fig. 12, c-d). Also in this case the curve relative to the treated zone reverses the trend in the drying phase, assuming greater values than the curve relative to the untreated zone. These graphs show how the water repellent in wall 1 keeps a thin film of drops of water over the surface, which slowly evaporate cooling the surface, unlike water repellent in wall 2.

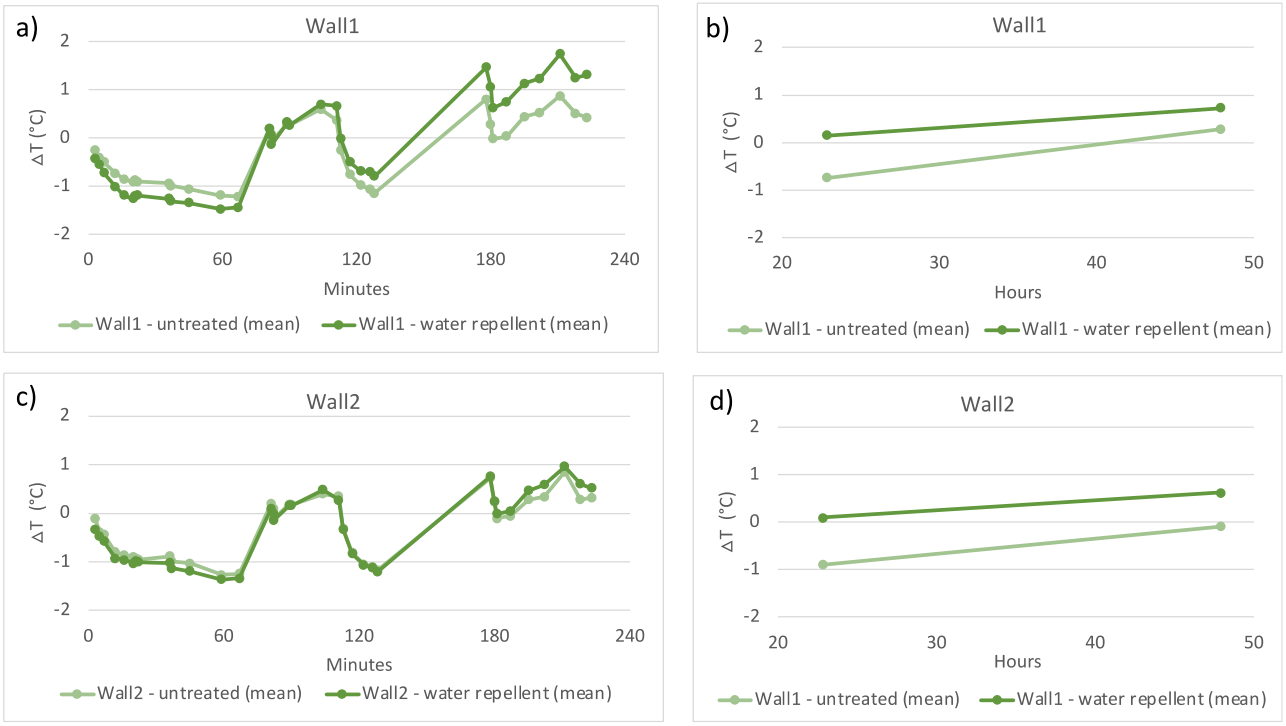

Figure 12. Mean ΔT values (°C) corrected to first acquisition value (dry wall) as a function of time (time 0 represents the end of wetting). External wetting of wall 1: in first 4 hours (a) and in the following days (b). External wetting of wall 2: in first 4 hours (c) and in the following days (d).

3.3 Tests on samples core-drilled from the brick walls

The capillary absorption coefficients of the brick cylinders (without mortar joints, as in Figure 6) are reported in Table 5. The difference between untreated and treated samples is similar to the one observed in the brick samples in Table 3, apart from some heterogeneity among the untreated bricks, which was ascribed to the variability characterizing this kind of material. Comparing the treatments applied onto the cylinders (Tab. 3, application by two brush strokes) and onto the walls (Tab. 5), the capillary absorption coefficient of water-repellent B is basically identical, while the capillary absorption coefficient of water-repellent A is a bit higher in the walls (~3 times as much), although still extremely limited.

Table 5. Capillary absorption coefficient (CA) of the brick cylinders core drilled from the walls.

Sample	CA ($mg/cm^2s^{1/2}$)	Mean CA value ($mg/cm^2s^{1/2}$)
1-UT	15.46	13.02±3.46
2-UT	10.57	
2-A-a	0.11	0.11±0.00
2-A-b	0.11	
1-B-a	0.11	0.12±0.01
1-B-b	0.12	

The penetration depth of the water repellents in the bricks was quite different, comparing the cylinders (Fig. 7) and the walls (Fig. 13):

- for the treatment A, the average penetration depth was 9 mm in the cylinders and 4 mm in the walls
- for the treatment B, the average penetration depth was 1 mm in the cylinders and 5 mm in the walls.

This was ascribed to the brushing application, which involves some unavoidable variability in the amount of water repellent absorbed by the substrate. However, these results suggest that the penetration depth does not influence so significantly the hydrophobic performance in the walls. In the core-drilled cylinders constituted by bricks and mortars, it can be observed that the water repellent penetrates a bit more in the mortar than in the bricks, likely due to its higher porosity.

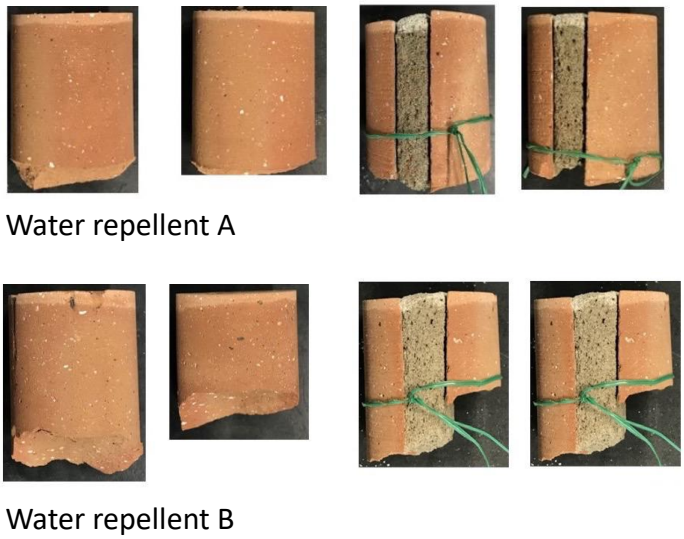

Figure 13. Penetration depth of the hydrophobic treatments observed by wetting the cylinders: a) samples treated with the product “A”; b) samples treated with the product “B”.

4. Conclusions

The results obtained in the present study allowed to derive the following conclusions:

- the penetration depth of water repellents into porous materials like brick and masonry is strongly influenced by the application method and by the volatility of the solvent;
- while the effectiveness of the water repellents in preventing rainwater absorption is good, almost independent on the penetration depth and easy to assess by simple experimental procedures, the drying behaviour of treated brick and masonry is more critical to evaluate;
- tests were carried out on brick cylinders wetted behind the treated face, simulating the occurrence of moisture from infiltration and/or condensation, and these highlighted that the drying rate is significantly affected by the treatments. In particular, the drying rate is much slower than the one expected on the basis of the standard wet cup test method, currently used to measure the coefficient of resistance to water vapour diffusion and hence the “breathability” of materials;

- tests were carried out on masonry walls purposely designed to investigate the behaviour in case of external and internal wetting, both during the wetting and drying phase. Active IR thermography allowed to follow the wetting and drying behaviour and to highlight aspects that were not visible at naked eye or with standard passive thermography. The mortar layers seemed to have no different influence of the hydric behaviour of the laboratory walls with respect to bricks;
- there is evidence that PCA highlights changes over time and therefore allows identification of areas with a greater temperature variation. It was also possible to detect defects in the water repellent treatments assessing the water absorption of the material and the speed of evaporation.

The results obtained via non-destructive and destructive testing of masonry walls in laboratory highlighted that the drying of water from walls is a slow process, which is significantly slowed down by surface treatments.

The methodology developed in this research is presently under testing in a real masonry building, where a water repellent treatment was applied to stop the brick deterioration. It will allow to collect important information about the actual behaviour of hydrophobic treatments onsite.

Acknowledgements

The present research has received funding from the national project IDEHA (Innovazioni per l'elaborazione dei dati nel settore del Patrimonio Culturale), within the "Programma Operativo Nazionale Ricerca e Innovazione 2014 – 2020" (MIUR - Ministero dell'istruzione, dell'università e della ricerca - Italy), Project N. ARS01_00421.

References

1. Doehne, E.; Price, C.A. *Stone conservation: an overview of current research.*; The Getty Conservation Institute: Los Angeles, 2010
2. van Hees, R.P.J. The performance of surface treatments for the conservation of historic brick masonry, Compat. Mater. Prot. Eur. Cult. Herit 2 (1998) 279–287
3. MacMullen, J., Radulovic, J., Zhang, Z., Dhakal, H. N., Daniels, L., Elford, J., ... & Bennett, N. (2013). Masonry remediation and protection by aqueous silane/siloxane macroemulsions incorporating colloidal titanium dioxide and zinc oxide nanoparticulates: Mechanisms, performance and benefits. Construction and Building Materials, 49, 93-100
4. Esposito Corcione, C.; Manno, R.; Frigione, M. Novel hydrophobic free solvent UV-cured hybrid organic-inorganic mathacrylic-based coatings for porous stones. Prog. Org. Coat. 2014, 77, 803–812
5. Toniolo, L., Casadio, F., Cariati, F. A key factor in modern protection of historic buildings: The assessment of penetration of water-repellent polymers into porous stone-materials. Annali di Chimica 91(11-12) (2001) 823-832
6. Schierhorn C. C., New thinking on water-repellent coatings for brick masonry. Masonry Construction the world of Masonry 9(4) (1996) 172-176
7. Feng, C.; Janssen, H. Impact of water repellent agent concentration on the effect of hydrophobization on building materials. J. Build. Eng. 39 (2021) 102284
8. Borsoi, G., Esteves, C., Flores-Colen, I., & Veiga, R. (2020). Effect of hygrothermal aging

on hydrophobic treatments applied to building exterior claddings. Coatings, 10(4), 363.
9. Esteves, C., Ahmed, H., Flores-Colen, I., & Veiga, R. The influence of hydrophobic protection on building exterior claddings. J. Coat. Technol. Res., 16 (5) 1379–1388, 2019
10. Emery, S. N. D., Charola, A. E. Coatings on brick masonry: are they protective or can they enhance deterioration? Journal of the American Institute for Conservation 46(1) (2007) 39-52
11. Slapø, F., Kvande, T., Bakken, N., Haugen, M., & Lohne, J. Masonry's Resistance to Driving Rain: Mortar Water Content and Impregnation. Buildings 7(3) (2017) 70
12. Lanteri P.C. Water-repellent coatings led to masonry damage. AFE Facilities Engineering Journal 25 (3) (1998) 17
13. Raupach, M., Wolff, L. Long-term durability of hydrophobic treatment on concrete. Surface Coatings International Part B: Coatings Transactions 88(2) (2005) 127-133
14. Manohar, S., Santhanam, M., Chockalingam, N. Performance and microstructure of bricks with protective coatings subjected to salt weathering. Construction and Building Materials 226 (2019) 94-105
15. Ioannou, I; Hoff, W D. Water repellent influence on salt crystallisation in masonry. Proceedings of the Institution of Civil Engineers - Construction Materials, 2008, Vol.161(1), p.17-23
16. Manohar, S., Santhanam, M. Assessing Efficiency of Protective Treatment Materials for Brick Structures. In: International Conference on Innovative Technologies for Clean and Sustainable Development (pp. 9-19). Springer, Cham, 2020
17. Zoghlami, K., Gómez-Gras, D., Álvarez, A., De Luxán, M. P. Evaluation of consolidating and water repellent treatments applied to the miocene sandstone used in Tunisian Heritage Monuments. Materiales de Construcción 55(277) (2005) 25-39
18. Martelli, M.; Salvatici, T.; Garzonio, C.A.; de Vita, M. Assessment of residual effectiveness for water-repellent treatments for building stones. Water absorption tests on the monumental complex Cathedral of San Zeno and the Baptistery of San Giovanni in Corte in Pistoia. *IOP Conf. Ser. Mater. Sci. Eng.* **2020**, *949*
19. Orlowsky, J., Braun F., Groh M. The influence of 30 years outdoor weathering on the durability of hydrophobic agents applied on Obernkirchener Sandstones. Buildings 10 (1) (2020) 1–18
20. Moreau, C.; Leroux, L.; Vergès-Belmin, V.; Fronteau, G. Which Factors Influence Most the Durability of Water Repellent Treatments: Stone Properties , Climate or Atmospheric Pollution? In Proceedings of the 5th International Conference on Water Repellent Treatment of Building Materials; 2008; pp. 129–142
21. Lazzarini, L.; Laurenzi Tabasso, M. Il restauro della pietra; Utet Scienze Tecniche, 2010
22. Schießl-Pecka A.A. Three examples of using hydrophobic impregnations in tunnels. fib Symposium 2016, p.1-7
23. Soulios, V., de Place Hansen, E. J., Peuhkuri, R., Møller, E., & Ghanbari-Siahkali, A. Durability of the hydrophobic treatment on brick and mortar. Building and Environment 201 (2021) 107994
24. Martelli, M., Worboys, M. J. Y., & Tesi, V. Monitoring and Conservation plans for monumental stone buildings. The case study of the Baptistery of San Giovanni in Corte in

Pistoia. IOP Conference Series: Materials Science and Engineering. Vol. 949. No. 1. IOP Publishing, 2020
25. Spodek, J.; Rosina, E. Application of infrared thermography to historic building investigation. J. Archit. Conserv. 2009, 15, 65–81, doi:10.1080/13556207.2009.10785040
26. Bauer, E.; Pavón, E.; Oliveira, E.; Pereira, C.H.F. Facades inspection with infrared thermography: cracks evaluation. J. Build. Pathol. Rehabil. 2016, 1, doi:10.1007/s41024-016-0002-9
27. Barreira, E.; Almeida, R.M.S.F.; Delgado, J.M.P.Q. Infrared thermography for assessing moisture related phenomena in building components. Constr. Build. Mater. 2016, 110, 251–269, doi:10.1016/j.conbuildmat.2016.02.026
28. Usamentiaga, R.; Venegas, P.; Guerediaga, J.; Vega, L.; Molleda, J.; Bulnes, F.G. Infrared thermography for temperature measurement and non-destructive testing. Sensors 2014, 14, 12305–12348
29. Nilsson, L.-O. *Methods of measuring moisture in building materials and structures*; Springer I.; 2018
30. Barbosa, M.T.G.; Rosse, V.J.; Laurindo, N.G. Thermography evaluation strategy proposal due moisture damage on building facades. *J. Build. Eng.* **2021**, *43*
31. Dafico, L.C.M.; Barreira, E.; Almeida, R.M.S.F.; Carasek, H. Comparison of infrared thermography and other traditional techniques to assess moisture content of wall specimens. Sensors 2022, 22, 3182
32. Proietti, N.; Calicchia, P.; Colao, F.; De Simone, S.; Di Tullio, V.; Luvidi, L.; Prestileo, F.; Romani, M.; Tatì, A. Moisture Damage in ancient masonry: A multidisciplinary approach for in situ diagnostics. Minerals 2021, 11, 406
33. Litti, G., Khoshdel, S., Audenaert, A., & Braet, J. (2015). Hygrothermal performance evaluation of traditional brick masonry in historic buildings. Energy and Buildings, 105, 393-411.
34. Rocha, J.H.A., Santos, C.F., Póvoas, Y.V. Evaluation of the infrared thermography technique for capillarity moisture detection in buildings. Procedia Structural Integrity 11 (2018) 107-113
35. Ghosh, D., Gupta, H., & Mittal, A. K. Non-destructive evaluation of historic masonry structures using infrared thermography and GPR. Lecture Notes in Mechanical Engineering 2022, p. 315-327
36. Olmi, R; Riminesi, C; Rosina, E. Integration of EFD, MRM and IRT for moisture mapping on historic masonry: Study cases in northern Italy. In Emerging technologies in nondestructive testing (ETNDT 6), pp. 471-476, Taylor & Francis
37. Jing T.S., Othuman Mydina M.A., Utaberta N. Appraisal of moisture problem of inheritance building envelope assemblies via visible and infrared thermography methods. Jurnal Teknologi 75 (5) (2015) 1 - 6
38. Grinzato, E.; Ludwig, N.; Cadelano, G.; Bertucci, M.; Gargano, M.; Bison, P. Infrared thermography for moisture detection: A laboratory study and in-situ test. Mater. Eval. 2011, 69, 97–104
39. Avdelidis, N.P.; Moropoulou, A. Applications of infrared thermography for the investigation of historic structures. J. Cult. Herit. 2004, 5, 119–127,

doi:10.1016/j.culher.2003.07.002
40. Sansonetti, A., Casati, M., Rosina, E., Gerenzani, F., Gondola, M., and Ludwig, N. Contribution of IR thermography to the performance evaluation of water repellent treatments. Restor. Build. Monum. 2012, 18, 13–22
41. Herrmann, T.D.; Mohamad, G.; Lima, R.C.A. de; Santos Neto, A.B. da S.; Lübeck, A. Estudo de caso do desempenho de estanqueidade à água de argamassas e hidrorrepelentes - Parte I. Matéria (Rio Janeiro) 2019, 24, doi:10.1590/s1517-707620190004.0841
42. Hu, Y.; Dong, Y.; Batunacun An automatic approach for land-change detection and land updates based on integrated NDVI timing analysis and the CVAPS method with GEE support. ISPRS J. Photogramm. Remote Sens. 2018, doi:10.1016/j.isprsjprs.2018.10.008
43. Bosc, M.; Heitz, F.; Armspach, J.-P.; Namer, I.; Gounot, D.; Rumbach, L. Automatic change detection in multimodal serial MRI: application to multiple sclerosis lesion evolution. Neuroimage 2003, 20, 643–656, doi:10.1016/S1053-8119(03)00406-3
44. Mas, J.-F. Monitoring land-cover changes: A comparison of change detection techniques. Int. J. Remote Sens. 1999, 20, 139–152, doi:10.1080/014311699213659
45. Jollife, I.T.; Cadima, J. Principal component analysis: A review and recent developments. Philos. Trans. R. Soc. A Math. Phys. Eng. Sci. 2016, 374, doi:10.1098/rsta.2015.0202
46. Minu, S.; Shetty, A. A Comparative Study of Image Change Detection Algorithms in MATLAB. Aquat. Procedia 2015, 4, 1366–1373, doi:10.1016/j.aqpro.2015.02.177
47. Radke, R.J.; Andra, S.; Al-Kofahi, O.; Roysam, B. Image change detection algorithms: A systematic survey. IEEE Trans. Image Process. 2005, 14, 294–307, doi:10.1109/TIP.2004.838698
48. Milovanović, B.; Gaši, M.; Gumbarević, S. Principal Component Thermography for Defect Detection in Concrete. Sensors 2020, 20, 3891
49. Trevisiol, F.; Barbieri, E.; Bitelli, G. Multitemporal Thermal Imagery Acquisition and Data Processing on Historical Masonry: Experimental Application on a Case Study. Sustainability 2022, 14, 10559
50. Ecem Edis, Inês Flores-Colen, Jorge de Brito, Quasi-quantitative infrared thermographic detection of moisture variation in facades with adhered ceramic cladding using principal component analysis, Building and Environment, Volume 94, Part 1, 2015, Pages 97-108, ISSN 0360-1323
51. EN 15801:2009. Conservation of cultural property - Test methods - Determination of water absorption by capillarity
52. Karagiannis, N., Karoglou, M., Bakolas, A., Krokida, M., & Moropoulou, A. (2017). Drying kinetics of building materials capillary moisture. Construction and Building Materials, 137, 441-449.
53. RILEM TC 25-PEM, Recommended tests to measure the deterioration of stone and to assess the effectiveness of treatment methods, Test No. II. 5 ‘‘Evaporation curve”, Mater. Struct. 13 (1980) 204–207
54. EN 16322, Conservation of Cultural Heritage – Test Methods – Determination of Drying Properties, 2013
55. ISO 12572, Hygrothermal performance of building materials and products — Determination of water vapour transmission properties — Cup method, 2016

56. EN 1015-19, Methods of test for mortar for masonry Part 19: Determination of water vapour permeability of hardened rendering and plastering mortars, 1998
57. Antolini, G.; Auteri, L.; Pavan, V.; Tomei, F.; Tomozeiu, R.; Marletto, V. A daily high-resolution gridded climatic data set for Emilia-Romagna, Italy, during 1961-2010. *Int. J. Climatol.* **2016**, *36*, 1970–1986
58. Ban, H.-J.; Kwon, Y.-J.; Shin, H.; Ryu, H.-S.; Hong, S. Flood Monitoring Using Satellite-Based RGB Composite Imagery and Refractive Index Retrieval in Visible and Near-Infrared Bands. Remote Sens. 2017, 9, 313. https://doi.org/10.3390/rs9040313
59. Franzoni E., Graziani G., Sassoni E., Bacilieri G., Griffa M., Lura P., Solvent based ethyl silicate for stone consolidation: influence of the application technique on penetration depth, efficacy and pore occlusion, Materials and Structures 48 (11) (2015) 3503-3515
60. Borsoi, G., et al., Effect of solvent on nanolime transport within limestone: How to improve in-depth deposition. Colloids and Surfaces A: Physicochemical and Engineering Aspects, 497 (2016) 171–181
61. Hall, C.; Hoff., W.D. *Water transport in brick, stone and concrete*; CRC, Ed.; London, 2021
62. Zhao, J.; Feng, S.; Grunewald, J.; Meissner, F.; Wang, J. Drying characteristics of two capillary porous building materials: Calcium silicate and ceramic brick. Building and Environment, 216, 2022, 109006
63. Cultrone, G., & Madkour, F. (2013). Evaluation of the effectiveness of treatment products in improving the quality of ceramics used in new and historical buildings. Journal of Cultural Heritage, 14(4), 304-310
64. S. Couto, T.D. Gonçalves, J.M.G. Lopes, Drying of red ceramic brick. Effect of five silicone-based water-repellent treatments, in: Hydrophobe VI, 6th Int. Conf. on Water Repellent Treatment of Building Materials, Istituto Superiore per la Conservazione ed il Restauro (ISCR), Rome, Italy, 2011, pp. 81–92